Original Paper

Tyrosine-Mutant AAV8 Vector Mediated Efficient and Safe Gene Transfer of Pigment Epithelium-Derived Factor to Mouse Lungs

Débora P. Ferreira[a,b,c]   Sabrina V. Martini[a]   Helena A. Oliveira[d]   Adriana L. Silva[a,b,c]
Siddharth Shenoy[f,g]   Daiqin Chen[f,g]   Valentina Simon[f]   Eric Han[f,g]
Natalie E. West[i]   Jung Soo Suk[f,g,h]   Patricia R.M. Rocco[b,c]   Hilda Petrs-Silva[e]
Marcelo M. Morales[a,c]   Fernanda F. Cruz[b,c]

[a]Laboratory of Cellular and Molecular Physiology, Carlos Chagas Filho Institute of Biophysics, Federal University of Rio de Janeiro, Rio de Janeiro, Brazil. [b]Laboratory of Pulmonary Investigation, Carlos Chagas Filho Institute of Biophysics, Federal University of Rio de Janeiro, Rio de Janeiro, Brazil. [c]National Institute of Science and Technology for Regenerative Medicine, Rio de Janeiro, RJ, Brazil. [d]Laboratory of Immunopharmacology, Oswaldo Cruz Institute, Fiocruz, Rio de Janeiro, Brazil. [e]Laboratory of Gene Therapy and Viral Vectors, Carlos Chagas Filho Institute of Biophysics, Federal University of Rio de Janeiro, Rio de Janeiro, Brazil. [f]Center for Nanomedicine, Wilmer Eye Institute, Johns Hopkins University School of Medicine, Baltimore, MD, USA. [g]Department of Ophthalmology, Johns Hopkins University School of Medicine, Baltimore, MD, USA. [h]Department of Chemical and Biomolecular Engineering, Whiting School of Engineering, Johns Hopkins University, Baltimore, MD, USA. [i]Department of Medicine, Johns Hopkins University, Baltimore, MD, USA.

Key Words

Abstract

Background/Aims: Recombinant adeno-associated viruses (rAAV) are an important tool for lung targeted gene therapy. Substitution of tyrosine with phenylalanine residues (Y-F) in the capsid have been shown to protect the AAV vector from ubiquitin/proteasome degradation, increasing transduction efficiency. We tested the mutant Y733F-AAV8 vector for mucus diffusion, as well as the safety and efficacy of pigment epithelium-derived factor (PEDF) gene transfer to the lung. ***Methods:*** For this purpose, Y733F-AAV8-PEDF (10^{10} viral genome) was administered intratracheally to C57BL/6 mice. Lung mechanics, morphometry, and inflammation were evaluated 7, 14, 21, and 28 days after injection. ***Results:*** The tyrosine-mutant AAV8 vector was efficient at penetrating mucus in *ex vivo* assays and at transferring the gene to lung cells after *in vivo* instillation. Increased levels of transgene mRNA were observed 28 days after vector administration. Overexpression of PEDF did not affect *in vivo*

M. M. Morales and F. F. Cruz contributed equally to this work.

Fernanda Ferreira Cruz

Carlos Chagas Filho Institute of Biophysics, University/Hospital: Federal University of Rio de Janeiro
Ilha do Fundão, Centro de Ciências da Saúde, Instituto de Biofísica Carlos Chagas Filho, Bloco G – 014, Rio de Janeiro, RJ, 21941-902, Brasil
Tel. +55 21 2562-6530, Fax +55 21 2280-8193, E-Mail ffcruz@biof.ufrj.br

Cellular Physiology and Biochemistry

Cell Physiol Biochem 2023;57:331-344

DOI: 10.33594/000000660
Published online: 18 September 2023

© 2023 The Author(s). Published by
Cell Physiol Biochem Press GmbH&Co. KG

332

Ferreira et al.: Y733F-AAV8 Vector is Safe and Effective For PEDF Gene Lung Delivery

lung parameters. ***Conclusion:*** These findings provide a basis for further development of Y733F-AAV8-based gene therapies for safe and effective delivery of PEDF, which has anti-angiogenic, anti-inflammatory and anti-fibrotic activities and might be a promising therapy for lung inflammatory disorders.

Introduction

Chronic respiratory diseases describe a range of diseases, including asthma, chronic obstructive pulmonary disease (COPD), idiopathic lung fibrosis, and occupational lung diseases, characterized by inflammation, oxidative stress, and eventually fibrosis of the airways and other pulmonary structures [1–3]. They are among the leading causes of mortality and morbidity worldwide [4]. Current treatments for some of these chronic respiratory diseases are still limited [5], thus, alternative therapeutic approaches that can attenuate both inflammatory and remodeling processes without leading to immunosuppression are required. In this context, gene therapy has emerged as a new strategy for the treatment of lung diseases refractory to conventional treatments. Innovative studies have been testing gene therapy using adeno-associated viral vectors (AAV), demonstrating efficient delivery of anti-inflammatory genes in murine models of chronic lung diseases [6–9].

AAV vectors are currently among the most frequently used viral vectors for gene therapy due to a combination of characteristics such as lack of pathogenicity, relatively low immunogenicity, a wide range of cell tropism, and induction of long-term gene expression. Moreover, AAV vectors have gained increasing popularity as a delivery gene transfer system since their approval by the US Food and Drug Administration for treatment of an inherited retinal disease and spinal muscular atrophy [10, 11]. Several approaches have been explored to improve the transduction efficiency of AAV vectors. It is known that, during intracellular trafficking to the cell nucleus, AAV vectors can undergo tyrosine kinase-phosphorylation/ubiquitination/proteasome-dependent degradation, which is a critical limitation of AAV-based vectors [12]. Previous studies have shown that site-specific point mutations that result in exchange of tyrosine residues with phenylalanine (Y-F) on AAV capsids protected vectors from destruction, resulting in increased transduction efficiency of the mutant relative to their wild-type counterparts, leading to enhanced transgene expression, both in cell cultures and in different animal tissues [13–17]. Of the 14 known serotypes of AAV (AAV1–9, 6.2, rh8, rh10, rh39, and rh43), AAV6, AAV8, and AAV9 have been shown to be the most efficient in delivering the gene to the airways, and AAV8 has the highest transgene expression in large airways [18, 19]. Thus, in this work, we chose the AAV8 mutant virus, in which the tyrosine residue was replaced by a phenylalanine at position 733 of the viral genome (Y733F-AAV8), to potentially enhance the efficacy as a vector for pulmonary gene transfer. In our previous work, we demonstrated that Y733F-AAV8 vectors displayed significantly increased transduction efficiency in the lung compared with their wild-type counterpart [15, 18].

In addition to improving AAV vectors, identifying therapeutic genes that can potentially reverse key pathology in chronic inflammatory/fibrotic lung diseases is crucial. In this context, pigment epithelium-derived factor (PEDF) is a promising therapeutic gene. Several studies have shown that PEDF has neurotrophic, neuroprotective, anti-inflammatory, anti-oxidative, anti-angiogenic, and anti-fibrotic properties [20–22]. Moreover, a previous study showed that intravenous administration of recombinant PEDF protein exerted significant anti-inflammatory and anti-remodeling effects in a murine model of chronic ovalbumin-induced asthma via suppression of VEGF. These positive results offered a potential treatment option for chronic airway inflammation diseases, even though protein-based therapy, unlike gene therapy, does not provide long-lasting therapeutic effects [23]. Therefore, in the present study, before investigating the potential of PEDF gene therapy in pulmonary diseases, we evaluated the diffusion of Y733F-AAV8 vector in mucus in an *ex vivo* assay, and the impact of administration of Y733F-AAV8 vector, carrying PEDF transgene or green fluorescent protein (GFP), as a control, at different time points after infection.

Cellular Physiology and Biochemistry

Cell Physiol Biochem 2023;57:331-344

DOI: 10.33594/000000660
Published online: 18 September 2023

© 2023 The Author(s). Published by
Cell Physiol Biochem Press GmbH&Co. KG

333

Ferreira et al.: Y733F-AAV8 Vector is Safe and Effective For PEDF Gene Lung Delivery

Materials and Methods

AAV viral vectors

Tyrosine-mutant Y733F-AAV8, obtained by site-directed mutation resulting in surface-exposed tyrosine (Y) exchanged by residues of phenylalanine (F) [15], was used in this study. Wild-type AAV2 and Y733F-AAV8 containing the gene for GFP were used in *ex vivo* sputum multiple particle tracking (MPT) to evaluate the vectors' ability to penetrate through the mucus barrier [24]. Y733F-AAV8, carrying either GFP or human PEDF, was used for *in vivo* studies. The expression of GFP and PEDF is driven by the strong small chicken β-actin promoter. All AAV vectors were provided by a former collaborator of the Retinal Gene Therapy Lab at University of Florida: Dr Hilda Petrs-Silva, Laboratory of Gene Therapy and Viral Vectors, Carlos Chagas Filho Biophysics Institute (IBCCF) of the Federal University of Rio de Janeiro (UFRJ).

Cystic fibrosis sputum sample collection

Cystic fibrosis *(*CF) sputum samples were collected with written informed consent in accordance with the Johns Hopkins Institutional Review Board (IRB) (NA_00046768). Spontaneously expectorated sputum samples were collected from patients visiting the Adult Cystic Fibrosis Center at Johns Hopkins University. MPT experiments were conducted using samples stored at 4°C immediately after collection for up to 24 h, based on previous confirmation that the barrier properties of freshly collected sputum are maintained under these conditions [24]. Patients involved in this study received no mucolytics other than Pulmozyme (i.e., dornase alfa) and/or hypertonic saline as part of their standard treatment regimen.

Multiple particle tracking in cystic fibrosis sputum

To determine if Y733F-AAV8 would be an efficient vector for gene therapy for inflammatory lung disease therapy, we assessed its ability to penetrate the human airway mucus barrier, measuring its diffusion rates in freshly collected sputum samples spontaneously expectorated by patients with CF via MPT. The motion of WT-AAV2 and Y733F-AAV8 in sputum was tracked by fluorescent video microscopy and quantified by MPT analysis using software custom-written in MATLAB (MathWorks, Natick, MA, USA), as previously reported [25]. For visualization and tracking of individual viruses, both AAVs were labeled with the amine-reactive fluorescent dye, Alexa Fluor 647 carboxylic acid succinimidyl ester (AF647; Life Technologies, Carlsbad, CA, USA), as previously described [26]. AF647-labeled AAVs were stored at −80°C and thawed on ice before use.

In vivo studies

This study was approved by the Ethics Committee of the Health Sciences Center (CEUA-CCS 050-14), Federal University of Rio de Janeiro and the Johns Hopkins University Animal Use and Care Committee (MO19M96). All animals received humane care in compliance with the *Principles of Laboratory Animal Care* formulated by the National Society for Medical Research and the *Guide for the Care and Use of Laboratory Animals* prepared by the National Academy of Sciences, USA. This study followed the ARRIVE guidelines for reporting of animal research.

Animals were housed at a controlled temperature (23°C) in a controlled light–dark cycle (12–12 h), with free access to water and food in the Laboratory of Cellular and Molecular Physiology and Laboratory of Pulmonary Investigation at Carlos Chagas Filho Institute of Biophysics (IBCCF) of the Federal University of Rio de Janeiro (UFRJ) and Miller Research Building bioterium of Johns Hopkins Hospital.

Intratracheal instillation

Female C57BL/6 mice (n=130) weighing between 20 and 25 g were used. Animals were anesthetized with inhaled sevoflurane and placed on a surgical table. An anterior longitudinal cervical incision of approximately 1 mm was made to expose the trachea. Vector or saline was instilled with a microsprayer (intratracheal aerosolizer; model S/M-551 1C DEA, PennCentury, Philadelphia, PA, USA) attached to a high-pressure syringe (model FMJ-250, PennCentury). The cervical incision was closed with 5.0 sutures and the animal returned to the cage.

GFP confocal imaging

To compare AAV vectors with regard to *in vivo* distribution of transgene expression in the lungs, 10 C57BL/6 mice received 50 µL of a solution of WT-AAV2 or Y733F-AAV8 (10^{10} intratracheally) packaged with a gene encoding GFP (WT-AAV2-GFP or Y733F-AAV8-GFP). Two weeks after administration, the animals were euthanized, the lungs were harvested, flash-frozen in optimum cutting temperature compound, and cryosectioned using a CM1950 cryostat (Leica Biosystems, Wetzlar, Germany). Slides were immunologically

Cellular Physiology
and Biochemistry

Cell Physiol Biochem 2023;57:331-344

DOI: 10.33594/000000660
Published online: 18 September 2023

© 2023 The Author(s). Published by
Cell Physiol Biochem Press GmbH&Co. KG

334

Ferreira et al.: Y733F-AAV8 Vector is Safe and Effective For PEDF Gene Lung Delivery

stained using DAPI (Sigma-Aldrich, St Louis, MO, USA) and subsequently imaged using a confocal LSM 510 microscope under 20× and 40× magnification. Four or more randomly selected image fields were taken from 3 lung tissue sections showing regions of the airways and airspace (i.e., a total of at least 12 images per animal) to quantify the distribution of transgene expression.

To quantitatively assess the distribution of GFP transgene expression in airways/airspace, the investigators were blinded and the airway regions were manually segmented using a threshold from the DAPI or blue channel in ImageJ (National Institutes of Health, USA). Using custom software written in Java, the boundaries of the airway and non-airway regions (i.e., anywhere outside selected airway regions) were further refined using automated image thresholding. The percentage of GFP coverage was defined as the GFP-positive airway/ airspace and cell area divided by the total area of a respective compartment. Before quantitative analysis, all images were normalized by fluorescence of untreated C57BL/6 lung tissue to eliminate the contribution of autofluorescence [24].

Experimental settings

To investigate the efficiency and safety of administration of the mutant AAV8 vector over time, 120 mice were randomly divided into 3 experimental groups with 40 animals per group (Fig. 1): (1) saline control group (CTRL), which received saline solution (NaCl 0.9%) intratracheally; (2) GFP group (GFP), treated intratracheally with 10^{10} copies of Y733F-AAV8 viral genome (vg) containing the gene encoding GFP protein; (3) PEDF group (PEDF), treated intratracheally with 10^{10} vg of Y733F-AAV8 containing the gene encoding human PEDF. Animals were then euthanized for analysis at 4 different time points (10 animals per group): 7 days (CTRL7d, GFP7d, PEDF7d), 14 days (CTRL14d, GFP14d, PEDF14d), 21 days (CTRL21d, GFP21d, PEDF21d), and 28 days (CTRL28d, GFP28d, PEDF28d), after instillation.
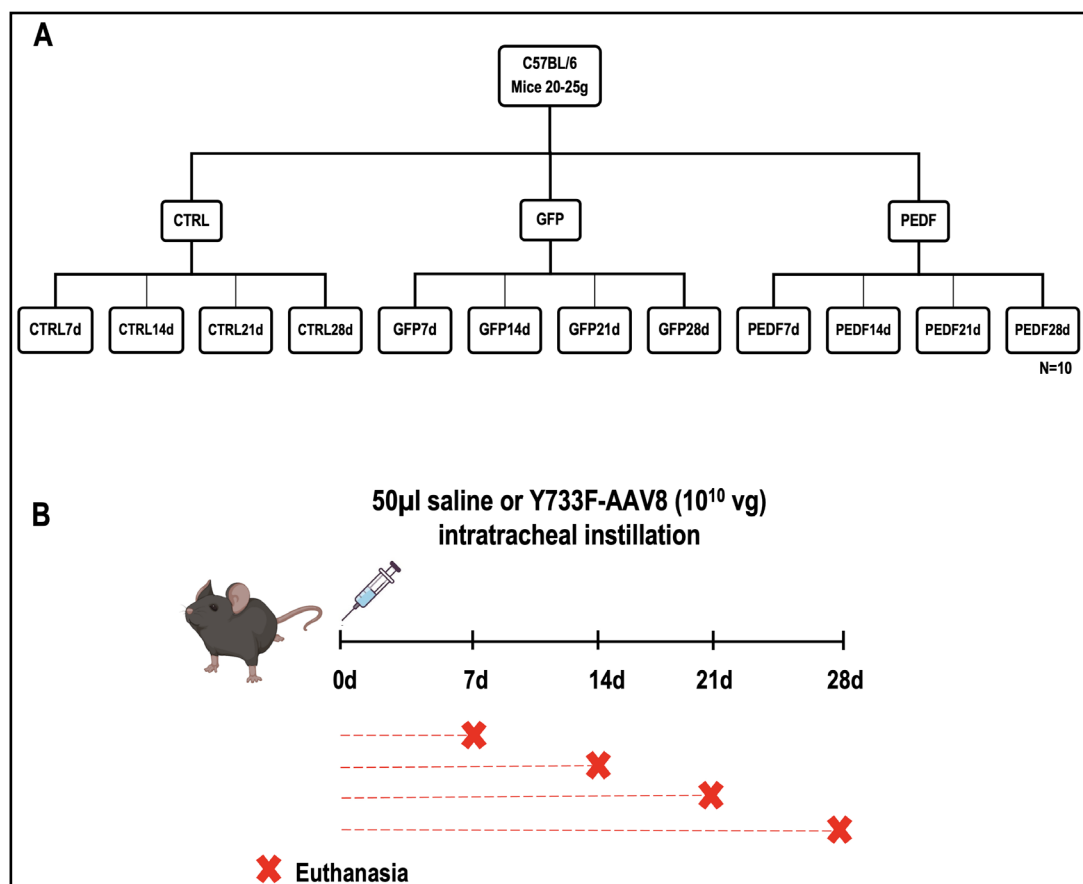
Fig. 1. Schematic representation of the experimental groups. A Mice were divided into 3 groups (n=40): control group (CTRL) and its subdivisions: CTRL7d, CTRL14d, CTRL21d, and CTRL28d (n=10); GFP group (GFP) and its subdivisions: GFP7d, GFP14d, GFP21d, and GFP28d (n=10); PEDF group (PEDF) and its subdivisions: PEDF7d, PEDF14d, PEDF21d, and PEDF28d (n=10); B Schematic representation of the experimental design. The animals received saline or Y733F-AAV8 vector virus on day zero and were harvested at 7, 14, 21 and 28 days after instillation.

Mechanical parameters

To evaluate lung function at different time points after instillation of Y733F-AAV8 vectors and overexpression of the transgenes, the pulmonary static elastance parameter (Est,L) was analyzed *in vivo*. Animals were sedated (diazepam 1 mg intraperitoneally), anesthetized (thiopental sodium 20 mg/kg intraperitoneally), tracheotomized, paralyzed (vecuronium bromide, 0.005 mg/kg intravenously), and ventilated with a constant flow ventilator (Samay VR15; Universidad de la República, Montevideo, Uruguay) with the following parameters: frequency, 100 breaths/min; tidal volume (V_T), 0.2 ml; and fraction of inspired oxygen, 0.21. The anterior chest wall was surgically removed, and a positive end-expiratory pressure of 2 cm H_2O was applied. Static lung elastance (Est, L) was determined [27–29]. Lung mechanics were measured 10 times in each animal. All data were analyzed using ANADAT data analysis software (RHTInfoData, Inc, Montreal, Quebec, Canada).

Lung histology

We analyzed lung morphometry and tissue cellularity at different time points to investigate whether the instillation of Y733F-AAV8-GFP or Y733F-AAV8-PEDF to the airways induced histologic changes in the lung. A laparotomy was done immediately after determining the lung mechanics, and heparin (1000 IU) was injected intravenously into the vena cava. The trachea was clamped at end expiration, and the animals were euthanized by exsanguination. The right lung was then removed, fixed in 3% buffered formaldehyde, and embedded in paraffin. Slices were cut (4 µm thick) and stained with hematoxylin–eosin. Lung histology analysis was performed with an integrated eyepiece using a coherent system consisting of a grid with 100 points and 50 lines (of known length) coupled to a conventional light microscope (Olympus BX51, Olympus Latin America, Brazil). The volume fraction of collapsed and normal pulmonary areas and the number of mononuclear and polymorphonuclear cells in the pulmonary tissue were determined using the point-counting technique across 10 random, non-coincident microscopic fields [30].

Real-time PCR

To establish the time course of transduction efficacy of Y733F-AAV8 vectors in the lung tissue after intratracheal instillation, a quantitative real-time reverse transcription polymerase chain reaction (PCR) was performed to measure the relative levels of mRNA of GFP (GFP; QIAGEN, Valencia, CA, USA), human and mouse PEDF (SERPIN1; QIAGEN) at different time points. Central slices of the left lung were cut, collected in cryotubes, quickly frozen by immersion in liquid nitrogen, and stored at −80°C. Total RNA was extracted from the frozen tissues using a RNeasy Plus Mini Kit (QIAGEN) according to the manufacturer's recommendations. The concentration of RNA was measured by spectrophotometry in Nanodrop ND-1000 (Thermo Scientific, Wilmington, DE, USA). First-strand cDNA was synthesized from total RNA using a QuantiTect Reverse Transcription Kit (QIAGEN). Relative mRNA levels were measured with an SYBR green detection system using Mastercycler ep realplex (Eppendorf, Hamburg, Germany). All samples were measured in triplicate. The mRNA level of each gene was calculated relative to the control gene (acidic ribosomal phosphoprotein P0; 36B4) as previously reported [15]. The $2^{-\Delta\Delta Ct}$ method was used to analyze the relative changes in gene expression from real-time quantitative PCR experiments.

Quantification of cytokines

Because PEDF has immuno-modulatory properties, we used ELISA to measure the expression of pro-inflammatory interleukin 6 (IL-6) and interleukin 1β (IL-1β), interferon gamma (IFN-γ), and monocyte chemoattractant protein-1 (MCP-1) in the lung tissue homogenate at different time points after Y733F-AAV8-PEDF instillation. For this purpose, the lung tissue was homogenized in lysis buffer (1 M sucrose, 1 M HEPES, 0.5 M EDTA, 200 mM NaF, 25× protease inhibitor (Roche, Basel, Switzerland), 200 mM PMSF) using a homogenizer (Tissue Lyser LT; QIAGEN, Hilden, Germany), subsequently centrifuged, and the supernatant was reserved and stored in a freezer at −80°C. The protein content of the samples was measured using the Bradford method; 3 µl of the samples was added to 197 µl of the reagent, in triplicate. The standard curve was performed with known concentrations of bovine albumin. The reaction was read at a wavelength of 595 nm. Levels of MCP-1, IL-6, IL-1β, and IFN-γ were measured with a Murine Mini ELISA Development Kit (Peprotech, Rocky Hill, NJ, USA), according to the manufacturer's protocol, and the absorbance reading was performed at a wavelength of 450 nm.

Statistical analysis

Data were analyzed with statistical tests, including Student's t test and a non-parametric Mann-Whitney test. Multiple comparisons were performed by one- and two-way analysis of variance, followed by the Bonferroni test. The parameters presented as percentages were subjected to arcsine transformation to make the distribution close to normal, thus allowing the variance tests to be performed [31]. Statistical analysis of the data was performed using GraphPad Prism 8 for Windows (V 3.0). Data were considered statistically significant when $P < 0.05$. The statistical tests used in each dataset are indicated in the figure legends.

Results

AAV particle tracking

The mutant vector, Y733F-AAV8, exhibited significantly greater diffusion rates, observed by its representative trajectory, and determined by mean squared displacement at a timescale of 1 s (MSD1s), compared with WT-AAV2, in 4 of 6 sputum samples collected from different patients with CF (Fig. 2A, B). MSD1s represents the average squared distance individual AAVs travel within a 1s time interval and is directly proportional to their diffusion rates [25].

AAV in vivo distribution

The lung distribution of GFP transgene expression was visualized 2 weeks post-infection, as shown in the representative confocal micrographs (Fig. 2C). The relative coverage of GFP expression was 6.4-fold greater when delivered by Y733F-AAV8, compared with WT-AAV2 ($P<0.05$; Fig. 2D). This result suggests that Y733F-AAV8 provides more widespread delivery of transgene payloads to the airways and lung cells.


Fig. 2. A AAV diffusion in spontaneously expectorated CF sputum. Box-and-whisker plots of MSD1 s of WT-AAV2 and Y733F-AAV8 in sputum samples collected from 6 individual patients with CF. Maximum whisker length is 1.5 times the interquartile range; outliers are shown as dots. WT-AAV2 vs. Y733F-AAV8; *P<0.0175; **P<0.0001; Mann-Whitney test. B Representative trajectories of WT-AAV2 and Y733F-AAV8 moving through CF sputum. The scale bar represents 200 nm. C AAV in vivo lung tissue distribution. In vivo AAV lung transgene distribution in mice after intratracheal administration of WT-AAV2 or Y733F-AAV8 (10^{10} vg/50 μl of saline). Representative images of GFP expression (green) in airways/airspace and cells. Confocal images of lung tissues from WT-AAV2- treated mice showing cell nuclei only (1) or with GFP transgene expression (2) and from Y733F-AAV8-treated mice showing cell nuclei only (3) or with GFP transgene expression (4). Cell nuclei are stained with DAPI (blue). The scale bar represents 100 μm. D Image-based quantification of GFP expression coverage is shown (n=3–4 mice with 3–4 lung sections per mouse). WT-AAV2 vs. Y733F-AAV8: *P<0.03; Student's t test.

Time course of transgene expression

GFP transgene expression was detected seven days after intratracheal injection, and there was a significant increment in GFP transcripts on day 28, corroborating that the peak expression occurred in the lung tissue 4 weeks after intratracheal instillation of Y733F-AAV8 (Fig. 3A). The expression of hPEDF transcript was detected as early as 7 days after intratracheal instillation, with peak expression at 28 days (Fig. 3B). Endogenous expression of the mouse PEDF (mPEDF) gene was observed in all experimental groups, with no statistical differences between them (Fig. 3C). Instillation of Y733F-AAV8-hPEDF did not interfere in the constitutive expression of the PEDF gene.
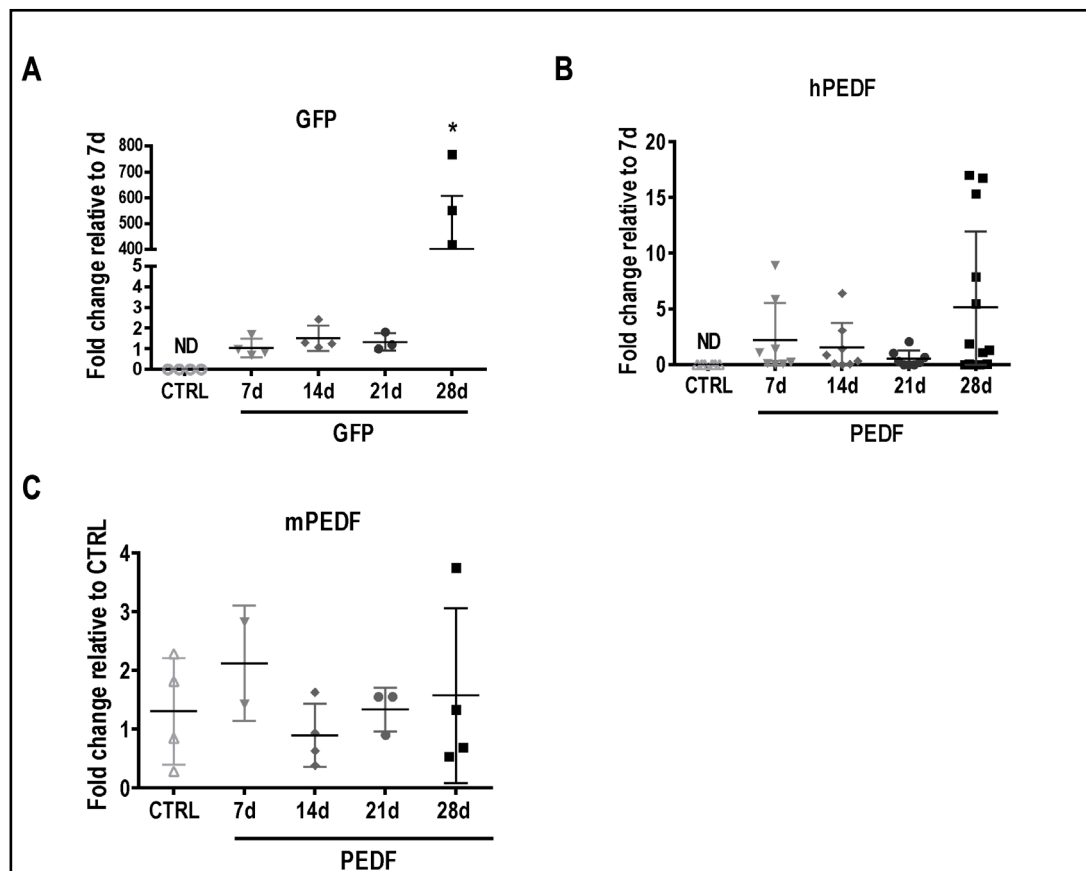
Fig. 3. Transgene in vivo lung expression. A GFP expression. Graph representing the relative mRNA levels of GFP. Animals were analyzed at 7 days, 14 days, 21 days, and 28 days after saline (CTRL, 50 μl of saline) or vector (Y733F-AAV8-GFP, 10^{10} vg/50 μl of saline) instillation. The y axis represents the level of eGFP gene calculated as the ratio of the housekeeping gene acidic ribosomal phosphoprotein P0 expression (36B4) relative to GFP7d. Values are means ± SD of 6–8 animals/group. *Significantly different from the 7d group ($P<0.05$); One-way ANOVA. B hPEDF expression. Graph representing the mRNA levels of hPEDF/36B4 relative to PEDF7d. The x axis represents the animals that were analyzed at 7, 14, 21, and 28 days after saline (CTRL, 50 μl of saline) or vector (Y733F-AAV8-PEDF, 10^{10} vg/50 μl of saline) instillation. Values are means ± SD of 6–8 animals/group. Values are not statistically different ($P>0.05$); One-way ANOVA followed by Bonferroni. C mPEDF expression. Graph representing the mRNA levels of mPEDF/36B4 genes relative to CTRL. The x axis represents the animals that were analyzed at 7, 14, 21, and 28 days after saline (CTRL, 50 μl of saline) or vector (Y733F-AAV8-PEDF, 10^{10} vg/50 μl of saline) instillation (n=6–8, mean±SD). Values are not statistically different ($P>0.05$); one-way ANOVA followed by Bonferroni.

338

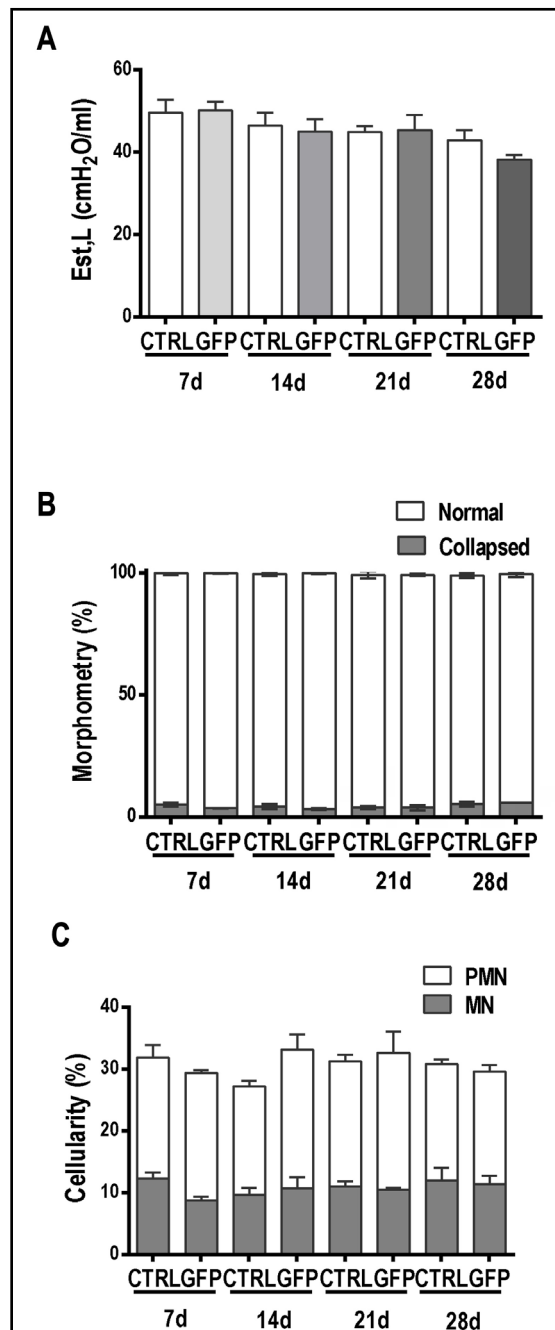Ferreira et al.: Y733F-AAV8 Vector is Safe and Effective For PEDF Gene Lung Delivery

Fig. 4. Lung function and morphology analyses (GFP). The x axis represents the animals that were analyzed at 7, 14, 21, and 28 days after saline (CTRL, 50 μl of saline) or vector (Y733F-AAV8-GFP, 10^{10} vg/50 μl of saline) instillation. A Static elastance (Est). The y axis represents the Est values. Values are means±SD of 6–8 animals/group. Values are not statistically different (P>0.05); Two-way ANOVA. B Morphometry. The y axis represents the percentage of normal and collapsed alveoli. The values correspond to the means±SD of 10 fields per slide, 6–8 slides per group; each animal is represented by only one slide. Values are not statistically different (P>0.05); Two-way ANOVA. C Cellularity. The percentages of mononuclear and polymorphonuclear cells are represented on the y axis. The values correspond to the means±SD of 10 fields per slide, 6–8 slides per group; each animal is represented by only one slide. Values are not statistically different (P>0.05); two-way ANOVA.
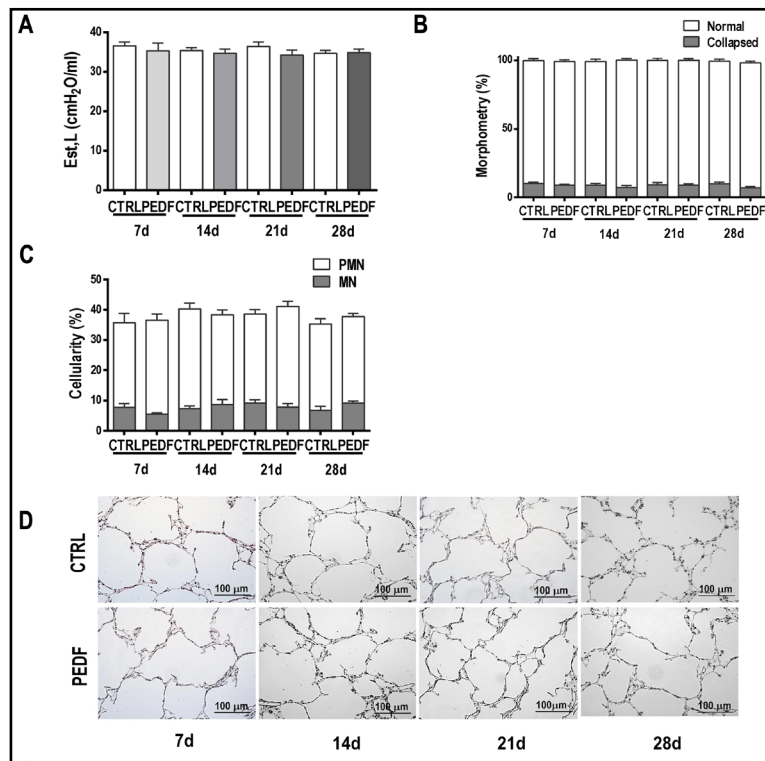

Pulmonary mechanics and histology

Est,L quantifies pulmonary resistance to volume change and the pressure required to overcome the resistive and elastic components of the lung. Est,L did not differ between the control and Y733F-AAV8-GFP groups (Fig. 4A) or the control and Y733F-AAV8-PEDF groups (Fig. 5A). The fractional area of collapsed alveoli (Figs. 4B and 5B), as well as the number of polymorpho- and mononuclear cells (Figs. 4C and 5C), did not differ between the groups. The administration of Y733F-AAV8 vector and the overexpression of PEDF transgene were safe and well tolerated.

Quantification of cytokines

The levels of MCP-1, IL-6, IL-1β, and IFN-γ were low and did not differ between the CTRL and PEDF groups at any time point (Fig. 6).

Cellular Physiology and Biochemistry

Cell Physiol Biochem 2023;57:331-344

DOI: 10.33594/000000660
Published online: 18 September 2023

© 2023 The Author(s). Published by
Cell Physiol Biochem Press GmbH&Co. KG

339

Ferreira et al.: Y733F-AAV8 Vector is Safe and Effective For PEDF Gene Lung Delivery

Fig. 5. Lung function and morphology analyses (PEDF). The x axis represents the animals that were analyzed at 7, 14, 21, and 28 days after saline (CTRL, 50 µl of saline) or vector (Y733F-AAV8-PEDF, 10^{10} vg/50 µl of saline) instillation. A Static elastance (Est). The y axis represents the elastance values. Values are means±SD of 6–8 animals/group (P>0.05); two-way ANOVA. B Morphometry. The y axis represents the percentages of normal and collapsed alveoli. The values correspond to the means±SD of 10 fields per slide, 6–8 slides per group; each animal is represented by only one slide. Values are not statistically different (P>0.05); two-way ANOVA. C Cellularity. The percentages of mononuclear and polymorphonuclear cells are represented on the y axis. The values correspond to the means±SD of 10 fields per slide, 6–8 slides per group; each animal is represented by only one slide. (P>0.05); two-way ANOVA. D Representative photomicrographs of lungs stained with hematoxylin–eosin on days 7, 14, 21, and 28. The scale bar represents 100 µm.
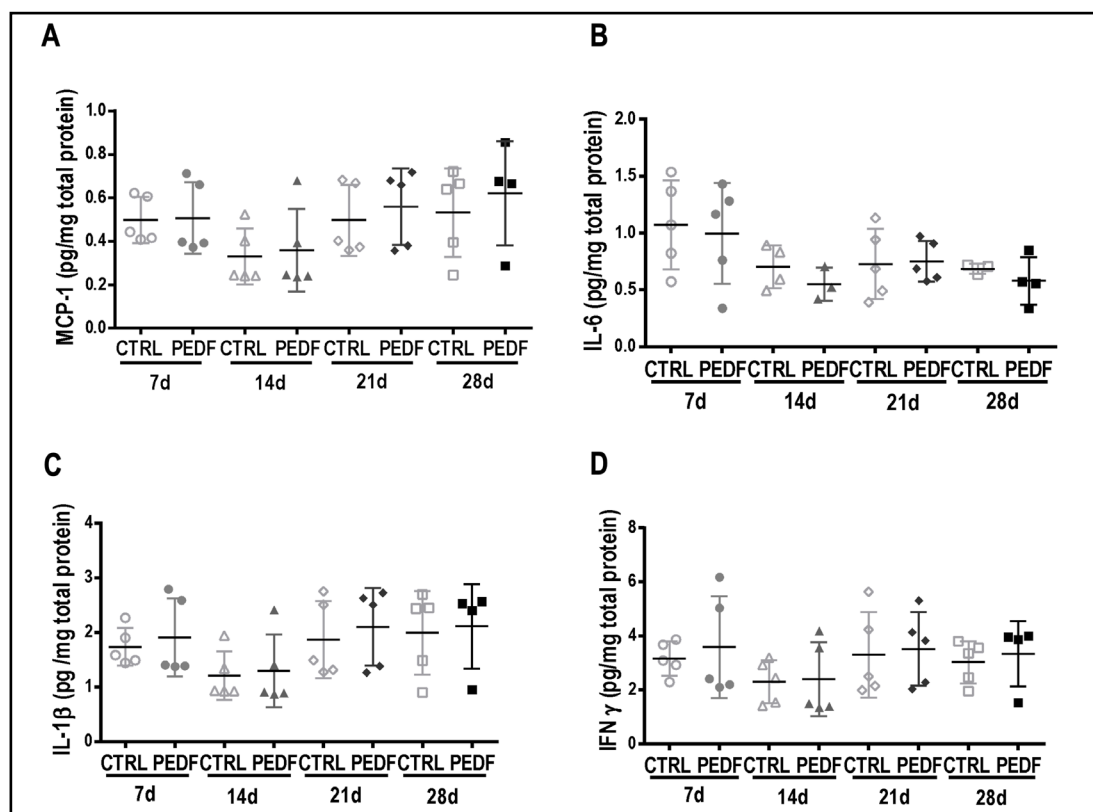
Fig. 6. Expression of inflammatory cytokines in the lung homogenate. Animals were analyzed at 7, 14, 21, and 28 days after instillation of saline (CTRL, 50 µl of saline) or vector (Y733F-AAV8-PEDF, 10^{10} vg/50 µl of saline). The y axis represents the cytokine expression values. Two-way ANOVA was used. A MCP-1. B IL-6.

Discussion

Although significant advancements with AAV vectors for lung gene therapy have been achieved, it is well recognized that challenges with AAV delivery, transduction, and induced immune responses need to be overcome for improved gene expression. For this reason, the safety and efficiency of AAV vectors have been studied for the treatment of lung diseases. In this work, we evaluated the mobility of Y733F-AAV8 in sputum from patients with CF *ex vivo* and its transduction efficiency over time *in vivo*, and investigated the impact of gene therapy on lung mechanics, histology, and inflammatory mediators.

It is known that AAV2, the most studied serotype and, therefore, the most used for gene delivery, is not efficient when transducing lung cells, because it binds primarily to the heparan sulfate proteoglycan (HSPG) receptor, which is poorly expressed in the apical membrane of these target cells [32]. It has been demonstrated that AAV serotype 8 is more effective in delivering the gene to such cells because it binds to the laminin receptor, which is abundantly expressed by epithelial lung cells [33]. To enhance AAV vector lung transduction efficiency, the use of a tyrosine to phenylalanine (Y-F) AAV capsid mutation has been studied [13, 14]. In a previous study, carried out by our group, it was shown that, compared with its wild-type (WT-AAV8), the Y733F-AAV8 mutant vector was more successful in transducing lung cells and did not show any evidence of inflammation [15] in healthy mice.

Patients with inflammatory lung diseases, such as asthma and CF, have increased mucus production [34]. The mucus network becomes a physical and chemical barrier for inhaled gene vectors, immobilizing and preventing them from reaching the target cells. In addition, mucus mesh facilitates removal of vectors from the airways via clearance mechanisms and is one of the greatest challenges in pulmonary gene therapy [24, 26]. Previous work has already demonstrated the inability of some adeno-associated virus, such as AAV2, AAV1 and AAV5 to efficiently traverse sputum samples from patients with CF, getting trapped in the mucin network [25, 26]. Hence, we evaluated the diffusion ability of the mutant AAV8 vector by MPT, using AAV2 for comparison purposes. This is the first time that a mutant Y733F-AAV8 was tested for mucus penetration. Our results showed that the Y733F-AAV8 vector exhibited significantly greater diffusion rates in sputum samples collected from different patients with CF compared with AAV2. This result shows that the Y733F-AAV8 vector can penetrate the mucus, suggesting that this vector could be efficient in crossing the mucus barrier and, therefore, delivering the gene to the lung cells of patients. We have also compared the distribution of these AAVs in lung tissue *in vivo*. For this, mice were instilled intratracheally with the vectors WT-AAV2 and Y733F-AAV8 carrying the GFP transgene. Animals that received the mutant AAV8 had a higher GFP covered area (55, 59%) compared with WT-AAV2 (8, 72%) and was therefore more efficient in delivering the reporter gene to mice lung cells *in vivo*.

The implications of PEDF gene therapy within normal lungs were not known. In the present study, we used the Y733F-AAV8 vector to deliver the transgenes PEDF and the control reporter gene, GFP, and analyzed the safety of PEDF overexpression and its importance for future gene therapy application for lung dysfunction. Several studies on gene therapy have used the PEDF gene because of its anti-inflammatory, anti-angiogenic, and anti-fibrotic properties, indicating that PEDF is a gene of interest for the treatment of COPD [20–23]. PEDF promoted the inhibition of nuclear factor kappa B (NFk-B), which induces the expression of various pro-inflammatory factors such as IL-6, IL-1β, MCP-1, and tumor necrosis factor alpha (TNF-α) in different disease models [35]. PEDF was also shown to have anti-oxidative properties, demonstrated by its ability to decrease the generation of reactive oxygen species, suppressing the activity of the enzymatic NADPH oxidase complex [36]. Other studies have shown that PEDF has an anti-angiogenic function with its ability to inhibit vascular endothelium growth factor, a potent angiogenic factor, which also promotes vascular permeability [37]. Moreover, PEDF exhibits anti-fibrotic activity by inhibiting TGF-β, and it inhibits the deposition of collagen induced by this factor [23]. Based on our results, we suggest that Y733F-AAV8 would be a promising vector for inflammatory lung disease

Cellular Physiology and Biochemistry

Cell Physiol Biochem 2023;57:331-344

DOI: 10.33594/000000660
Published online: 18 September 2023

© 2023 The Author(s). Published by
Cell Physiol Biochem Press GmbH&Co. KG

341

Ferreira et al.: Y733F-AAV8 Vector is Safe and Effective For PEDF Gene Lung Delivery

therapy. However, it is still necessary to evaluate PEDF expression, over time, regarding lung structure, inflammation, and mechanics.

In this work, the presence of human PEDF mRNA was detected as early as 7 days after intratracheal instillation, with a peak expression at 28 days, corroborating the data obtained with GFP vector and data from other authors [15]. Since a surge is seen in transgene expression on day 28, new studies testing therapeutic approaches using Y733F-AAV8-PEDF should take this time response in consideration, in order to evaluate possible therapeutic impact of therapy in later time points, when biological effects related to the transgene expression may happen.

Since both human and mouse PEDF can act on the same receptor, and overexpression of human PEF could possibly regulate endogenous PEDF expression, we have also analyzed the mouse expression of the PEDF gene in mouse lungs. All animals had endogenous expression of mouse PEDF gene, and there was no significant difference between the groups, indicating that the overexpression of PEDF did not interfere with the constitutive expression of mouse PEDF through real-time PCR analysis of the lung tissue.

It is well known that pulmonary gene therapy using viral vectors can induce immune reactions that can lead to disrupted lung morphometry and alterations in lung mechanics [38–40]. In this study, the fractional area of collapsed alveoli, as well as the total cellularity analysis, did not show significant differences between the experimental groups. Therefore, the results of the morphologic analysis of the pulmonary parenchyma suggest that the administration of Y733F-AAV8 vector and the transduction of the PEDF gene did not cause histologic changes indicative of inflammation. Another important indication of inflammation is the presence of inflammatory cytokines [41]. Analysis of the pro-inflammatory cytokines IL-1β, IL-6, IFN-γ, and the MCP-1 chemokine, using the ELISA technique, besides presenting low expression, did not show a significant difference in normal lungs at different times after PEDF overexpression (PEDF7d, PEDF14d, PEDF21d, PEDF28d) and in their respective controls.

Inflammation may be associated with the remodeling process, which involves replacement of the tissue damaged by fibrosis [42]. Furthermore, evidence suggests that airway remodeling can lead to changes in the intrinsic mechanical properties of the lung parenchyma with progressive loss of lung function [43, 44]. To evaluate the impact of administration of Y733F-AAV8 vector and transgene GFP and PEDF overexpression on lung function, pulmonary mechanics were analyzed using the end-of-inspiration occlusion method proposed by Bates et al [27–29].. An increase in Est,L indicates the presence of edema, alveolar collapse, and pulmonary fibrosis, consequent to the attempt at tissue repair [30, 45, 46]. However, the lung mechanics did not differ between the groups, suggesting that both Y733F-AAV8 vector and overexpression of hPEDF gene did not cause damage to lung function.

Conclusion

In summary, this study has demonstrated the repercussions of the overexpression of PEDF over time through the Y733F-AAV8 viral vector on the function and inflammatory pattern of airways and pulmonary parenchyma in mice after intratracheal instillation. Administration of Y733F-AAV8-PEDF vector was efficient in delivering the transgene to the pulmonary cells; did not lead to changes in lung function; did not cause histologic alterations suggestive of inflammation in lung parenchyma; and did not trigger the expression of inflammatory cytokines. These findings provide motivation for the further development of viral-based therapies with PEDF transgene for the treatment of respiratory diseases with inflammation and fibrosis, such as silicosis and asthma.

Cellular Physiology and Biochemistry

Cell Physiol Biochem 2023;57:331-344

DOI: 10.33594/000000660
Published online: 18 September 2023

© 2023 The Author(s). Published by
Cell Physiol Biochem Press GmbH&Co. KG

342

Ferreira et al.: Y733F-AAV8 Vector is Safe and Effective For PEDF Gene Lung Delivery

Disclosure Statement

The authors have no competing interests to declare.

References

1   Corlateanu A, Mendez Y, Wang Y, Garnica RJA, Botnaru V, Siafakas N: Chronic obstructive pulmonary disease and phenotypes: a state-of-the-art. Pulmonology 2020;26:95–100.

2   Ritchie AI, Wedzicha JA: Definition, causes, pathogenesis, and consequences of chronic obstructive pulmonary disease exacerbations. Clin Chest Med 2020;41:421-438.

3   Agusti A, Faner R: Chronic obstructive pulmonary disease pathogenesis. Clin Chest Med 2020;41:307–314.

4   Soriano JB, Kendrick P, Paulson K, Gupta V, Vos T, the GBD Chronic Respiratory Disease Collaborators: Prevalence and attributable health burden of chronic respiratory diseases, 1990–2017: a systematic analysis for the Global Burden of Disease Study 2017. Lancet Respir Med 2020;8:585–596.

5   Brandsma CA, Van den Berge M, Hackett TL, Brusselle G, Timens W: Recent advances in chronic obstructive pulmonary disease pathogenesis: from disease mechanisms to precision medicine. J Pathol 2020;250:624–635.

6   Wu CJ, Chen LC, Huang WC, Chuang CL, Kuo ML: Alleviation of lung inflammatory responses by adeno-associated virus 2/9 vector carrying CC10 in OVA-sensitized mice. Hum Gene Ther 2013;24:48–57.

7   Wu CJ, Huang WC, Chen LC, Shen CR, Kuo ML: Pseudotyped adeno-associated virus 2/9-delivered CCL11 shRNA alleviates lung inflammation in an allergen-sensitized mouse model. Hum Gene Ther 2012;23:1156–1165.

8   Strobel B, Duechs MJ, Schmid R, Stierstorfer BE, Bucher H, Quast K, Stiller D, Hildebrandt T, Mennerich D, Gantner F, Erb KJ, Kreuz S: Modeling pulmonary disease pathways using recombinant adeno-associated virus 6.2. Am J Respir Cell Mol Biol 2015;53:291–302.

9   Smalley E: First AAV gene therapy poised for landmark approval. Nat Biotechnol 2017;35:998–999.

10 Kuzmin DA, Shutova MV, Johnston NR, Smith OP, Fedorin VV, Kukushkin YS, van der Loo JCM, Johnstone EC: The clinical landscape for AAV gene therapies. Nat Rev Drug Discov 2021;20:173–174.

11   Keeler AM, Flotte TR: Recombinant Adeno-Associated Virus Gene Therapy in Light of Luxturna (and Zolgensma and Glybera): Where Are We, and How Did We Get Here? Annu Rev Virol 2019;6:601–621.

12   Zhong L, Zhao W, Wu J, Li B, Zolotukhin S, Govindasamy L, Agbandje-McKenna M, Srivastava A: A dual role of EGFR protein tyrosine kinase signaling in ubiquitination of AAV2 capsids and viral second-strand DNA synthesis. Mol Ther 2007;14:1079–1088.

13   Zhong L, Li B, Jayandharan G, Mah CS, Govindasamy L, Agbandje-Mckenna M, Srivastava A: Tyrosine-phosphorylation of AAV2 vectors and its consequences on viral intracellular trafficking and transgene expression. Virology 2008;381:194–202.

14   Zhong L, Li B, Mah CS, Govindasamy L, Agbandje-Mckenna M, Cooper M, Herzog RW, Zolotukhin I, Warrington KH Jr, Weigel-Van Aken KA, Hobbs JA, Zolotukhin S, Muzyczka N, Srivastava A: Next generation of adeno-associated virus 2 vectors: point mutations in tyrosines lead to high-efficiency transduction at lower doses. Proc Natl Acad Sci USA 2008;105:7827–7832.

15   Martini SV, Da Silva AL, Ferreira D, Gomes K, Ornellas FM, Lopes-Pacheco M, Zin E, Petrs-Silva H, Rocco PR, Morales MM: Single tyrosine mutation in AAV8 vector capsid enhances gene lung delivery and does not alter lung morphofunction in mice. Cell Physiol Biochem 2014;34:681–690.

16   Martini SV, Silva AL, Ferreira D, Rabelo R, Ornellas FM, Gomes K, Rocco PR, Petrs-Silva H, Morales MM: Tyrosine mutation in AAV9 capsid improves gene transfer to the mouse lung. Cell Physiol Biochem 2016;39:544–553.

17   van Lieshout, LP, Domm, JM, Rindler, TN, Frost, KL, Sorensen, DL, Medina, SJ, Booth, SA, Bridges, JP, Wootton, SK: A Novel Triple-Mutant AAV6 Capsid Induces Rapid and Potent Transgene Expression in the Muscle and Respiratory Tract of Mice. Mol Ther Methods Clin Dev 2018;9:323–329.

18   Lopes-Pacheco M, Kitoko JZ, Morales MM, Petrs-Silva H, Rocco PRM: Self-complementary and tyrosine-mutant rAAV vectors enhance transduction in cystic fibrosis bronchial epithelial cells. Exp Cell Res 2018;372:99–107.

19   McClain LE, Davey MG, Zoltick PW, Limberis MP, Flake AW, Peranteau WH: Vector serotype screening for use in ovine perinatal lung gene therapy. J Pediatr Surg 2016;51:879–884.

20   Tombran-Tink J, Johnson LV: Neuronal differentiation of retinoblastoma cells induced by medium conditioned by human RPE cells. Invest Ophthalmol Vis Sci 1989;30:1700–1707.

21   Tombran-Tink J, Chader GG, Johnson LV: PEDF: a pigment epithelium-derived factor with potent neuronal differentiative activity. Exp Eye Res 1991;53:411–414.

22   Shin ES, Sorenson CM, Sheibani N: PEDF expression regulates the proangiogenic and proinflammatory phenotype of the lung endothelium. Am J Physiol Lung Cell Mol Physiol 2014;306:L620–L634.

23   Zha W, Su M, Huang M, Cai J, Du Q: Administration of pigment epithelium-derived factor inhibits airway inflammation and remodeling in chronic OVA-induced mice via VEGF suppression. Allergy Asthma Immunol Res 2016;8:161–169.

24   Duncan GA, Kim N, Colon-Cortes Y, Rodriguez J, Mazur M, Birket SE, Rowe SM, West NE, Livraghi-Butrico A, Boucher RC, Hanes J, Aslanidi G, Suk JS: An adeno-associated viral vector capable of penetrating the mucus barrier to inhaled gene therapy. Mol Ther Methods Clin Dev 2018;9:296–304.

25   Schuster BS, Ensign LM, Allan DB, Suk JS, Hanes J: Particle tracking in drug and gene delivery research: state-of-the-art applications and methods. Adv Drug Deliv Rev 2015;91:70–91.

26   Schuster BS, Kim AJ, Kays JC, Kanzawa MM, Guggino WB, Boyle MP, Rowe SM, Muzyczka N, Suk JS, Hanes J: Overcoming the cystic fibrosis sputum barrier to leading adeno-associated virus gene therapy vectors. Mol Ther 2014;22:1484–1493.

27   Bates JH, Decramer M, Chartrand D, Zin WA, Boddener A, Milic-Emili J: Volume-time profile during relaxed expiration in the normal dog. J Appl Physiol 1985;59:732–737.

28   Bates JH, Ludwig MS, Sly PD, Brown K, Martin JG, Fredberg JJ: Interrupter resistance elucidated by alveolar pressure measurement in open-chest normal dogs. J Appl Physiol 1988;65:408–414.

29   Bates JH, Rossi A, Milic-Emili J: Analysis of the behavior of the respiratory system with constant inspiratory flow. J Appl Physiol 1985;58:1840–1848.

30   Weibel ER: Morphometry: stereological theory and practical methods; in: Gil J (ed): Models of Lung Disease Microscopy and Structural Methods. Marcel Dekker, New York, 1990:pp. 199–247.

31   Zar Jerrold H: Data transformations in Lynch D (ed): Biostatistical Analysis; 5th ed. Pearson Prentice Hall, Upper Saddle River, New Jersey, 2010:291–294.

32   Griesenbach U, Geddes DM, Alton EW: Gene therapy for cystic fibrosis: an example for lung gene therapy. Gene Ther 2004;1:S43–S50.

33   Liqun WR, Mclaughlin T, Cossette T, Tang Q, Foust K, Campbell-Thompson M, Martino A, Cruz P, Loiler S, Mueller C, Flotte TR: Recombinant AAV serotype and capsid mutant comparison for pulmonary gene transfer of alpha-1-antitrypsin using invasive and noninvasive delivery. Mol Ther 2009;17:81–87.

34   Fahy JV, Dickey BF: Airway mucus function and dysfunction. N Engl J Med 2010;363:2233–2247.

35   Ide Y, Matsui T, Ishibashi Y, Takeuchi M, Yamagishi S: Pigment epithelium-derived factor inhibits advanced glycation end product-elicited mesangial cell damage by blocking NF-kappaB activation. Microvasc Res 2010;80:227–232.

36   Yamagishi S, Inagaki Y, Nakamura K, Abe R, Shimizu T, Yoshimura A, Imaizumi T: Pigment epithelium-derived factor inhibits TNF-alpha-induced interleukin-6 expression in endothelial cells by suppressing NADPH oxidase-mediated reactive oxygen species generation. J Mol Cell Cardiol 2004;37:497–506.

37   Wang X, Xiu P, Wang F, Zhong J, Wei H, Xu Z, Liu F, Li J: P18 peptide, a functional fragment of pigment epithelial-derived factor, inhibits angiogenesis in hepatocellular carcinoma via modulating VEGF/VEGFR2 signaling pathway. Oncol Rep 2017;38:755–766.

38   Zhou Q, Chen T, Bozkanat M, Ibe JC, Christman JW, Raj JU, Zhou G: Intratracheal instillation of high dose adenoviral vectors is sufficient to induce lung injury and fibrosis in mice. PLoS One 2014;9:e116142.

39   Lassance RM, Pássaro CP, Martini SV, Castiglione RC, Gutierrez TM, Abreu SC, Antunes MA, Xisto DG, Cebotaru L, Petrs-Silva H, Zin WA, Guggino WB, Linden R, Rocco PR, Morales MM: Does the use of recombinant AAV2 in pulmonary gene therapy damage lung function? Respir Physiol Neurobiol 2008;160:91–98.

40   Martini SV, Fagundes SS, Schmidt AC, Avila M, Ornellas DS, Ribas VT, Petrs-Silva H, Linden R, Faffe DS, Guggino SE, Rocco PR, Zin WA, Morales MM: Does the use of recombinant AAV5 in pulmonary gene therapy lead to lung damage? Respir Physiol Neurobiol 2009;168:203–209.

41   Mesquita Júnior D, Araújo JA, Catelan TT, Souza AW, Cruvinel WDeM, Andrade LE, Silva NP: Immune system - part II: basis of the immunological response mediated by T and B lymphocytes. Rev Bras Reumatol 2010;50:552–580.

42   Rocco PR, Negri EM Kurtz PM, Vasconcellos FP, Silva GH, Capelozzi VL, Romero PV, Zin WA: Lung tissue mechanics and extracellular matrix remodeling in acute lung injury. Am J Respir Crit Care Med 2001;164:1067–1071.

43   Xisto DG, Farias LL, Ferreira HC, Picanço MR, Amitrano D, Lapa E Silva JR, Negri EM, Mauad T, Carnielli D, Silva LF, Capelozzi VL, Faffe DS, Zin WA, Rocco PR: Lung parenchyma remodeling in a murine model of chronic allergic inflammation. Am J Respir Crit Care Med 2005;171:829–837.

44   Da Silva AL, Martini SV, Abreu SC, Samary C Dos S, Diaz BL, Fernezlian S, de Sá VK, Capelozzi VL, Boylan NJ, Goya RG, Suk JS, Rocco PR, Hanes J, Morales MM: DNA nanoparticle-mediated thymulin gene therapy prevents airway remodeling in experimental allergic asthma. J Control Release 2014;180:125–133.

45   Rubini A, Carniel EL: A review of recent findings about stress-relaxation in the respiratory system tissues. Lung 2014;192:833–839.

46   Rubini A: The effects of prone with respect to supine position on stress relaxation, respiratory mechanics, and the work of breathing measured by the end-inflation occlusion method in the rat. Lung 2015;194:53–59.